LITERATURE CITED

(1) Arbuzov, B. A., Vinogradova, V. S., *Izvestiya Akad. Nauk. S.S.S.R., Otdel. Khim. Nauk* **1952**, 882-93.
(2) Burger, L. L., "Uranium and Plutonium Extraction by Organo-Phosphorus Compounds," *J. Phys. Chem.* **62**, 590 (1958).
(3) Burger, L. L., Forsman, R. C., "Solubility of Tributyl Phosphate in Aqueous Solutions," General Electric Co., Hanford Laboratories, Richland, Wash. **HW-20936** (April 2, 1951).
(4) Daasch, L. W., Smith, D. C., "Infrared Spectra of Phosphorus Compounds," NRL Rept. **3657** (April 1950); *Anal. Chem.* **23**, 853 (1951).
(5) Evans, D. P., *J. Chem. Soc.* **1930**, 1310.
(6) Ford-Moore, A. H., Williams, J. H., *J. Chem. Soc.* **1947**, 1465.
(7) Kabachnik, N. I., Rossiiskaya, P. A., *Bull. Acad. Sci., U.R.S.S., Classe Sci. Chim.* **1945**, 364.
(8) Kosolapoff, G. M., *J. Am. Chem. Soc.* **64**, 2982 (1942).
(9) *Ibid.*, **67**, 1180 (1945).
(10) *Ibid.*, **69**, 1002 (1947).
(11) Kosolapoff, G. M., "Organophosphorus Compounds," Wiley, New York, 1950.
(12) Kosolapoff, G. M., Alabama Polytechnic Institute, Auburn, Ala.; private communication.
(13) Kosolapoff, G. M., U. S. Patent **2,594,454** (April 29, 1952).
(14) Kosolapoff, G. M., McCullough, J. F., *J. Am. Chem. Soc.* **73**, 5392 (1951).
(15) Kosolapoff, G. M., Watson, R. M., *Ibid.*, **73**, 4101 (1951).
(16) Meyrick, C., Thompson, H. W., *J. Chem. Soc.* **1950**, 225.
(17) Noller, C. R., Dutton, G. R., *J. Am. Chem. Soc.* **55**, 424 (1933).
(18) Toy, A. D. F. (to Victor Chemical Co.), U. S. Patent **2,400,577** (May 21, 1946).
(19) Williams, R. H., Hamilton, L. A., *J. Am. Chem. Soc.* **74**, 5418 (1952).

Received for review November 22, 1957. Accepted April 30, 1958. Northwest Regional Meeting, ACS, Pullman, Wash., June 1953. Work was included in paper by L. L. Burger, B. R. Jones, and R. M. Wagner.

Infrared Emission Spectra of Two-Stage Hydrocarbon Flames

KENNETH WARK, Jr., and JOHN T. AGNEW
Mechanical Engineering Department, Purdue University, West Lafayette, Ind.

WILLIAM G. AGNEW
Fuels and Lubricants Department, General Motors Corp., Detroit, Mich.

For solving modern combustion problems, the role of chemical reaction kinetics must be further examined and developed. In such processes as autoignition in Diesel engines and preignition and knock in spark-ignition engines, it is highly probable that low temperature reactions have an effect. These reactions in many instances give rise to visible flames termed cool and/or two-stage flames, the temperatures of which may be on the order of 200° to 500° C. in the case of the first-stage or cool flame and 800° to 1200° C. for the second-stage flame.

A number of investigators have proposed chemical reaction theories which attempt to outline the reactions that lead up to and follow cool flame formation. Insight into the reaction mechanisms comes largely from fundamental experimental data which will validate or void previous hypotheses. Up to the present time the great majority of data supporting various proposed mechanisms has been obtained by wet chemical methods. These methods have the disadvantage that the products of combustion must be removed from the experimental apparatus for chemical analysis. In most cases this requires a change in sample temperature and pressure, and considerable time may be required for sampling and analysis. As a result, the chemical constituents determined in the sample could be different qualitatively and quantitatively from those actually existent in the reaction.

One of the most useful means of studying cool flame reactions with no external disturbance is by spectroscopic techniques coupled with a flat-flame burner. Spectroscopic analysis may utilize either emission spectra of thermally

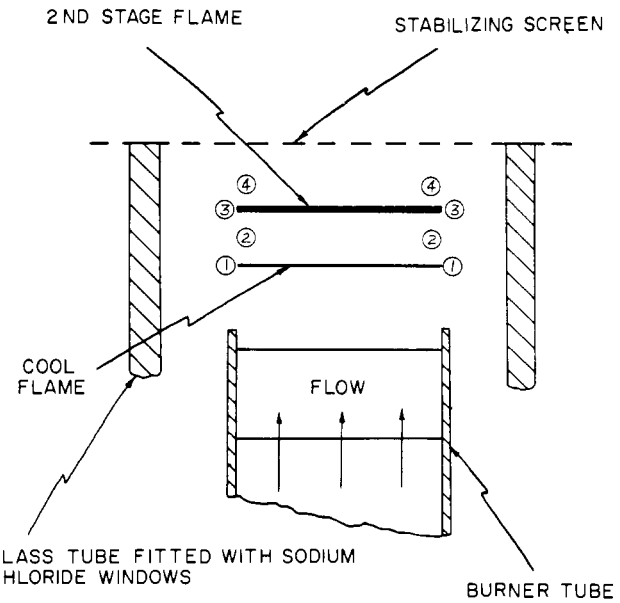

Figure 1. Diagrammatic sketch of two-stage flat flame

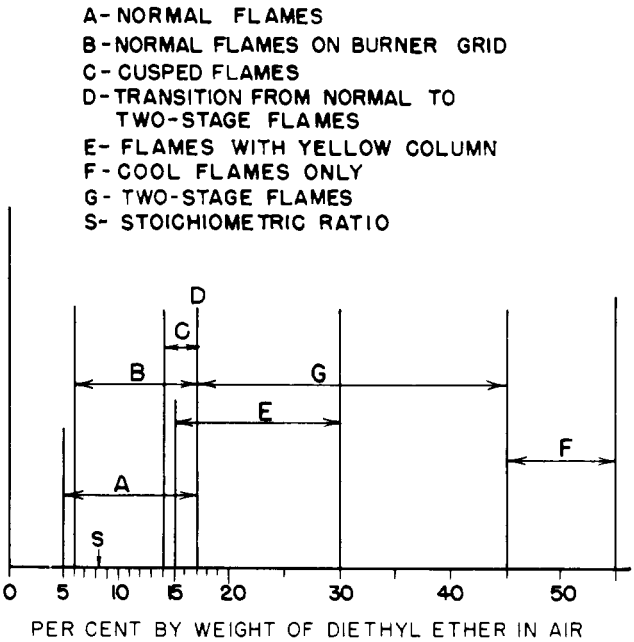

Figure 2. Flame structure at various fuel-air ratios

excited chemical species or absorption spectra of normal and/or excited molecules. This optical procedure allows detection of transient molecular species without their removal from the experimental apparatus and without quenching the reaction at an intermediate stage.

Only infrared emission spectral data are reported here. Results of a similar study in the visible spectral range were presented previously (*1*) with a full discussion of the characteristics of two-stage flat flames. Infrared spectra of two-stage ether flames have been reported (*2*) and are repeated here for a convenient comparison with the emission spectra of ether and the other two fuels, acetaldehyde and *n*-heptane. The ether spectra were also investigated at the Research Laboratories of General Motors Corp. (*4*); there more emphasis was placed on the temperature and spectral emissivity of the various stages of the low temperature reactions. The primary purpose of this study is to show that spectral radiation studies are capable of showing significant differences in intermediate species present with respect to fuel type.

APPARATUS

The two-stage flames were produced in a flat-flame burner similar to that described by Powling (*7*) and modified by Egerton and Thabet (*5*). The usual parabolic velocity distribution in a cylindrical flow passage is altered to a flat (uniform velocity) distribution by use of several layers of glass helices and nickel matrices. The nickel matrix in this case divided a brass burner tube 2 inches in diameter into parallel flow passages, each passage being about $^1/_{32}$ inch in diameter.

On the top of the burner was placed a square enclosure which provided a region where the desired flames could be stabilized without outside disturbances; sodium chloride windows 2 inches in diameter were inserted on opposite sides of the square enclosure. While one window permitted infrared radiation to pass from the flame into the optical system, the opposite window minimized background radiation. The center portion of the 10-inch-long burner tube was wrapped with asbestos sheeting and resistance wiring for heating the fuel-air mixture. It was necessary to heat *n*-heptane–air mixtures to around 200° C. before cool flames could be produced at atmospheric pressure. Figure 1 is a sketch of the flame zone of the flat-flame burner, indicating the position of the stabilized flame zones which are numbered to correspond to the spectra shown in later figures.

The fuel-air mixture supplied to the burner was prepared by bubbling air through containers of liquid fuel. This con-

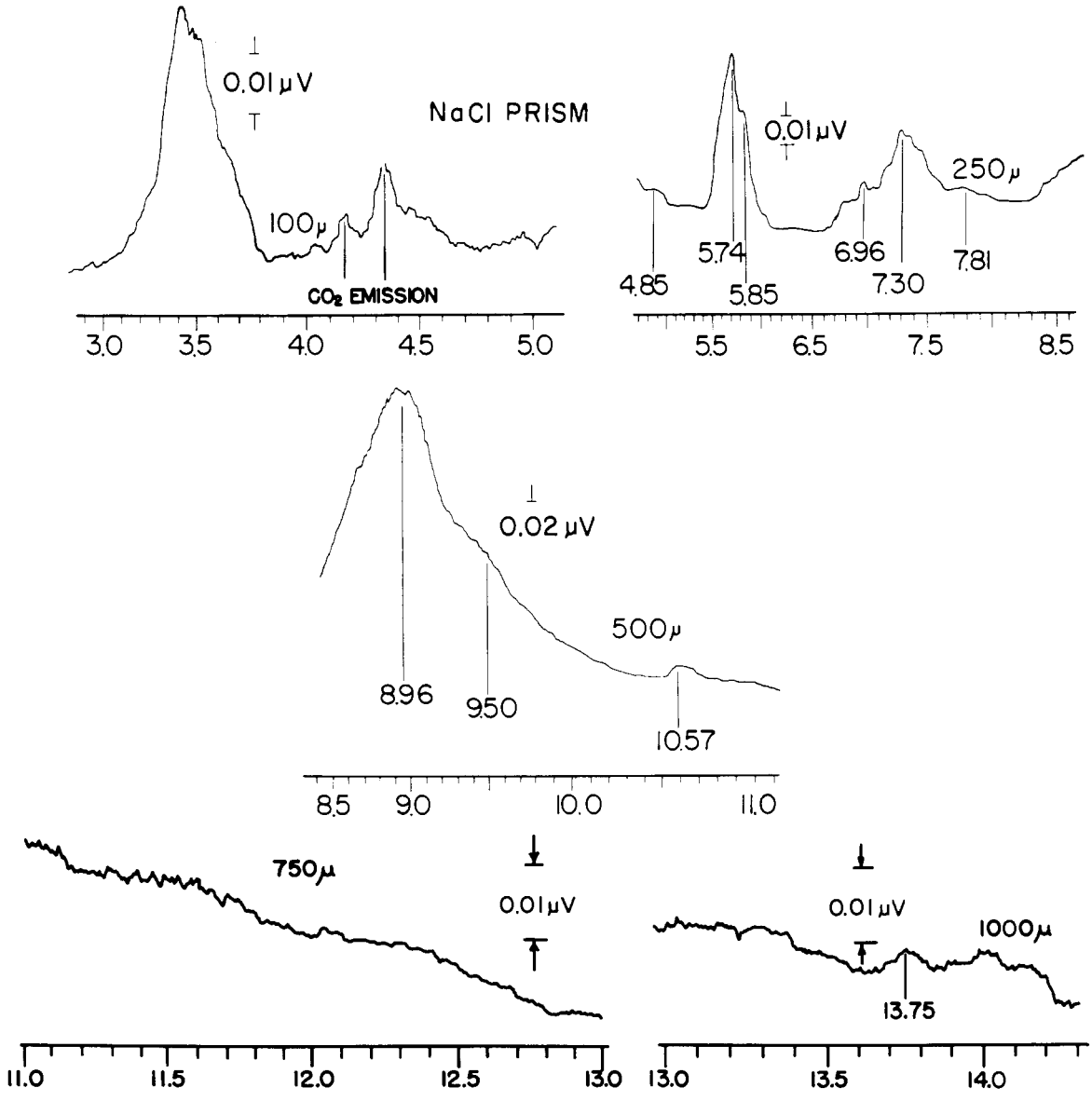

Figure 3. Emission spectrum of diethyl ether–air first-stage cool flame from 2.9 to 14.0 microns

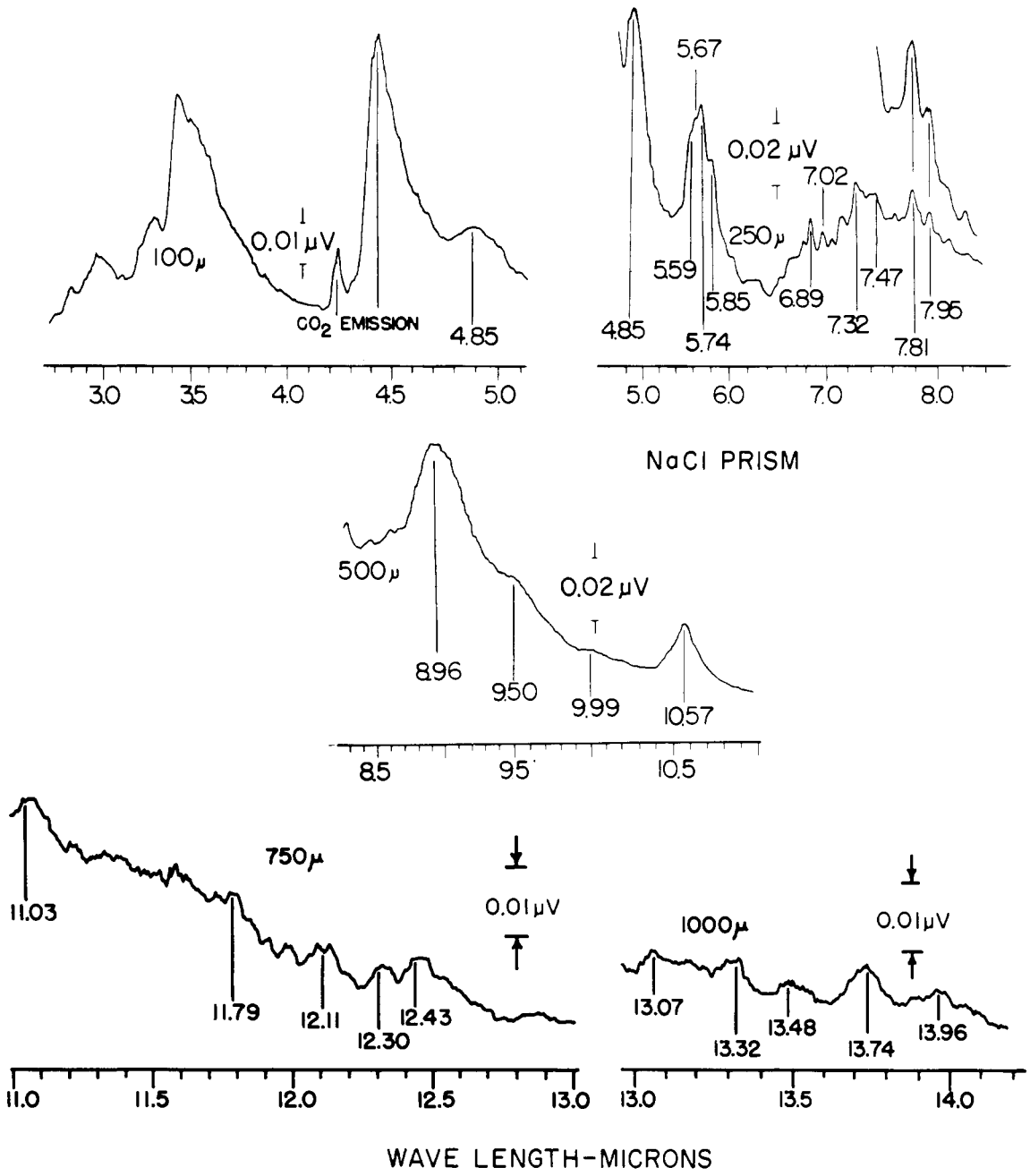

Figure 4. Emission spectrum of diethyl ether-air second-stage flame from 2.7 to 14.0 microns

tact-evaporating system established a fairly well saturated gaseous fuel-air mixture.

The optical system for the measurement of infrared radiation provided means for focusing radiation from a portion of the two-stage flames on the slit of a commercial double-pass infrared monochromator. Both lithium fluoride and sodium chloride prisms were used in the monochromator to obtain the maximum resolving power in the various spectral ranges studied. The prism type and slit width used to obtain the various spectra are indicated in Figures 3 to 15, inclusive. The external focusing device consisted of a spherical mirror and two plane mirrors so positioned that a horizontal section of the flame appeared in a vertical position at the entrance slit of the monochromator. Tests indicated that the horizontal strip of combustion area being viewed by the monochromator was about $\frac{1}{8}$ to $\frac{3}{16}$ inch thick by 0.25 inch long. The distances between combustion stages were sufficient to permit viewing only a single stage at a time.

The radiation signal picked up by the thermocouple in the monochromator was fed through a preamplifier and amplifier and finally recorded on a strip chart recorder as a function of wave length. No attempt was made to evaluate the magnitude of background radiation. The use of sodium chloride windows on both ends of the flame region minimized background radiation, but a small amount was undoubtedly present.

The spectra shown in Figures 3 to 15 are reproductions of the actual curves obtained on the strip chart recorder. The ordinates are thus only a qualitative indication of relative intensity of the various emission bands. Consideration must be given to the slit width and amplifier gain used, which are indicated on the various curves, to obtain even a qualitative comparison of absolute intensities of the various emission bands.

VARIATION OF FLAME STRUCTURE WITH FUEL-AIR RATIO

Various types of flame structure may be formed in a flat-flame burner, depending on the fuel-air ratio. The structure of diethyl ether flames was examined from around 5 to over

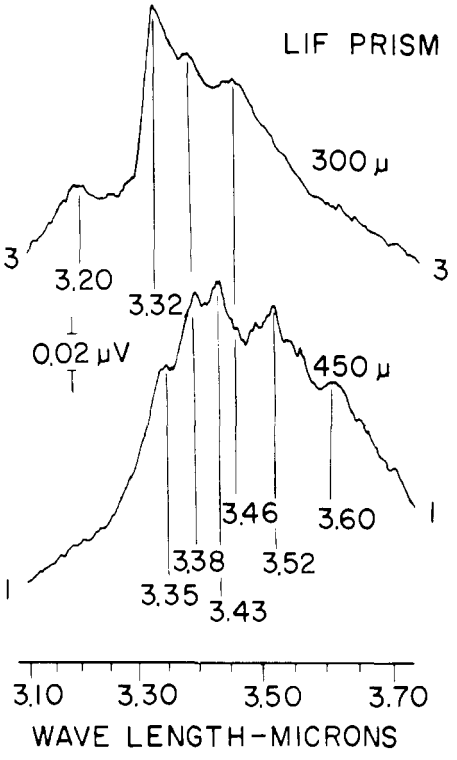

Figure 5. Emission spectra of diethyl ether-air two-stage flame from 3.1 to 3.7 microns

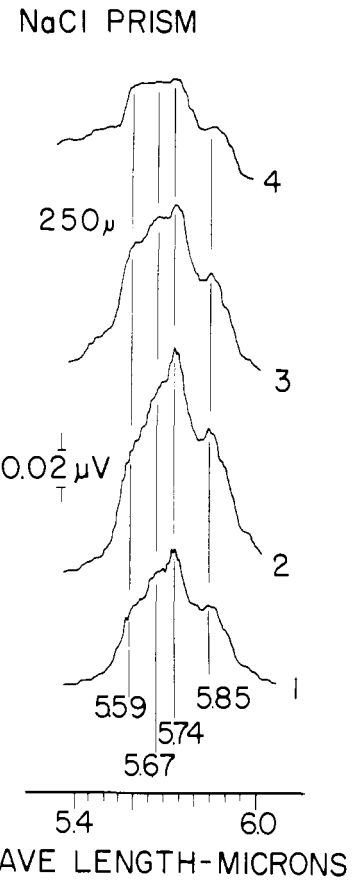

Figure 6. Emission spectra of diethyl ether-air two-stage flame from 5.4 to 6.0 microns

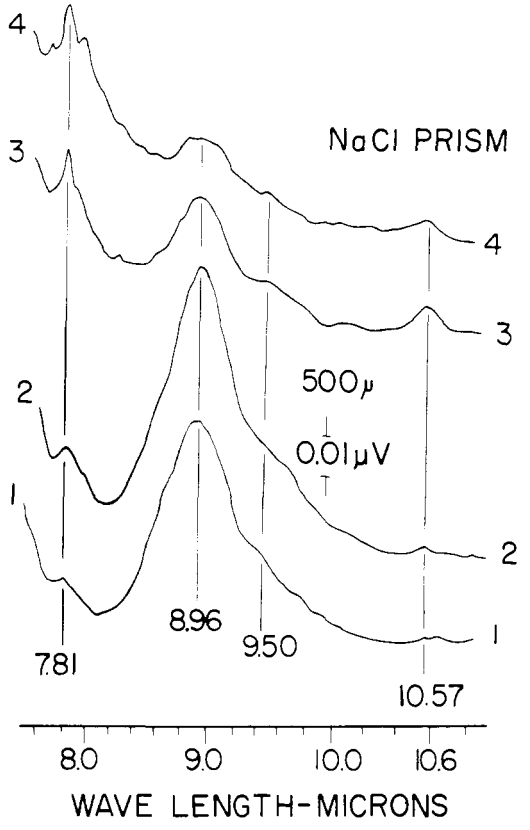

Figure 7. Emission spectra of diethyl ether-air two-stage flame from 7.6 to 10.8 microns

50 weight % ether. For acetaldehyde and *n*-heptane data were taken only in the region of the two-stage flame formation.

Variation in flame structure with diethyl ether as the fuel as a function of fuel-air ratio has been discussed extensively (*1*). Figure 2 is a summary of the types of flames obtained. With ether as the fuel, incipient formation of two-stage flames occurred at about 17% fuel (*D*, Figure 2). At almost imperceptibly richer mixtures a separation occurred between the first-stage cool flame and what has been termed the second-stage flame. The second-stage flame under some conditions appears to constitute a second cool flame and under other conditions has a character all its own. The transition of the rich normal flame to the two-stage flame as the mixture is enriched is characterized by a transition in the visible emission spectrum from the usual C_2, OH, CH spectrum to a formaldehyde luminescence spectrum in the first-stage cool flame and a predominantly HCO spectrum in the second-stage flame.

Results for acetaldehyde indicate that incipient formation of two-stage flames occurred at about 20.7 weight % of fuel. In the case of *n*-heptane, two-stage flames were formed at a fuel content of about 19%.

RESULTS AND DISCUSSION

The three fuels—diethyl ether, acetaldehyde, and *n*-heptane—were chosen because they represented three distinct types of organic compounds that form two-stage flames readily at atmospheric pressure.

Spectral results are presented in two forms. The first-stage cool flame and second-stage spectra for each fuel are shown for the entire spectral range. In addition, particular regions of the spectrum have been studied in greater detail. In Figures 5, 6, 7, 10, 11, 14, and 15, position 1-1 designates "in the first-stage cool flame zone." Position 3-3 denotes the "second-stage flame zone." Position 2-2 lies between the first and second stages, and position 4-4 above the second stage. This numbering system corresponds to that shown in Figure 1.

The spectra shown in Figures 3 and 4 are composite infrared emission spectra from diethyl ether first-stage and second-stage flames, respectively. Similar spectra are shown in Figures 8 and 9 for acetaldehyde and in Figures 12 and 13 for *n*-heptane.

Figures 5, 6, and 7 are detailed studies of particular spectral ranges for diethyl ether flames. Similarly, Figures

10 and 11 are detailed studies with acetaldehyde, while Figures 14 and 15 are detailed studies for *n*-heptane.

Spectral Range 3.0 to 4.0 Microns. It is difficult to identify or even detect the presence of transient product molecules by means of their characteristic emission spectra in the C — H stretching range shown in Figures 5, 10, and 14. Because the fuels containing C — H bonds are in excess in all cases, all spectra will contain a wide variety of C — H stretching radiations arising from the original fuels and numerous intermediate and final products of pyrolysis and oxidation. Nevertheless, distinct differences in the C — H stretching bands of Figures 5, 10, and 14, indicate differences in the reactions for the three fuels.

The band peaks near 3.21 and 3.32 microns occurring with all three fuels are apparently due to C — H stretching vibrations in unsaturated molecules (*3*, *6*). For all three fuels the emission from unsaturates is stronger in the second-stage flame than in the first-stage cool flame. Of the three fuels, acetaldehyde, which contains a carbon-oxygen double bond itself, showed the strongest unsaturate emission, diethyl ether had the next strongest emission, and *n*-heptane the weakest.

The CH_3 group stretching frequency would be expected to result in two emission peaks at 3.36 to 3.39 and 3.47 to 3.49 microns (*3*). Because all three fuels contain this grouping, and certain of their degradation products would also contain it, it is not surprising that emission peaks appeared in all of the spectra at one or both of these wave length regions.

The CH_2 group is present in two of the fuels and probably also in the degradation products of the third fuel, acetaldehyde, so again it is not surprising that emission peaks occur in most of the spectra at one or both of the two CH_2 stretching group frequencies, 3.40 to 3.43 and 3.49 to 3.52 microns (*3*). Diethyl ether (Figure 5) presents an interesting case because the CH_2 emission is particularly distinct in the first-stage cool flame but appears to be absent from the second-stage flame spectrum.

The tertiary CH group stretching frequency gives weak absorption in the 3.45 to 3.47 micron region (*3*) and thus might be expected to show some emission in all of the spectra in this region.

The CH stretching vibration in the H — C = O group gives absorption in the 3.45 to 3.70 micron region (*3*), and emission in the burner spectra near 3.6 microns may very well arise from vibrations in this group. The acetaldehyde first-stage cool flame spectrum (Figure 10) shows the strongest 3.6 micron emission, which might be expected since H — C = O appears in the original fuel. With diethyl ether (Figure 5) and *n*-heptane (Figures 12 and 13) emission near 3.6 microns is probably not from the fuel but due to formaldehyde or acetaldehyde formed as an intermediate product. In both of these latter cases the emission in this region is weaker in the second stage than in the first-stage cool flame, indicating consumption of the aldehydes. Evidence is presented later, with diethyl ether as the fuel, that formaldehyde concentration is greater in the second-stage flame than in the first-stage cool flame, so

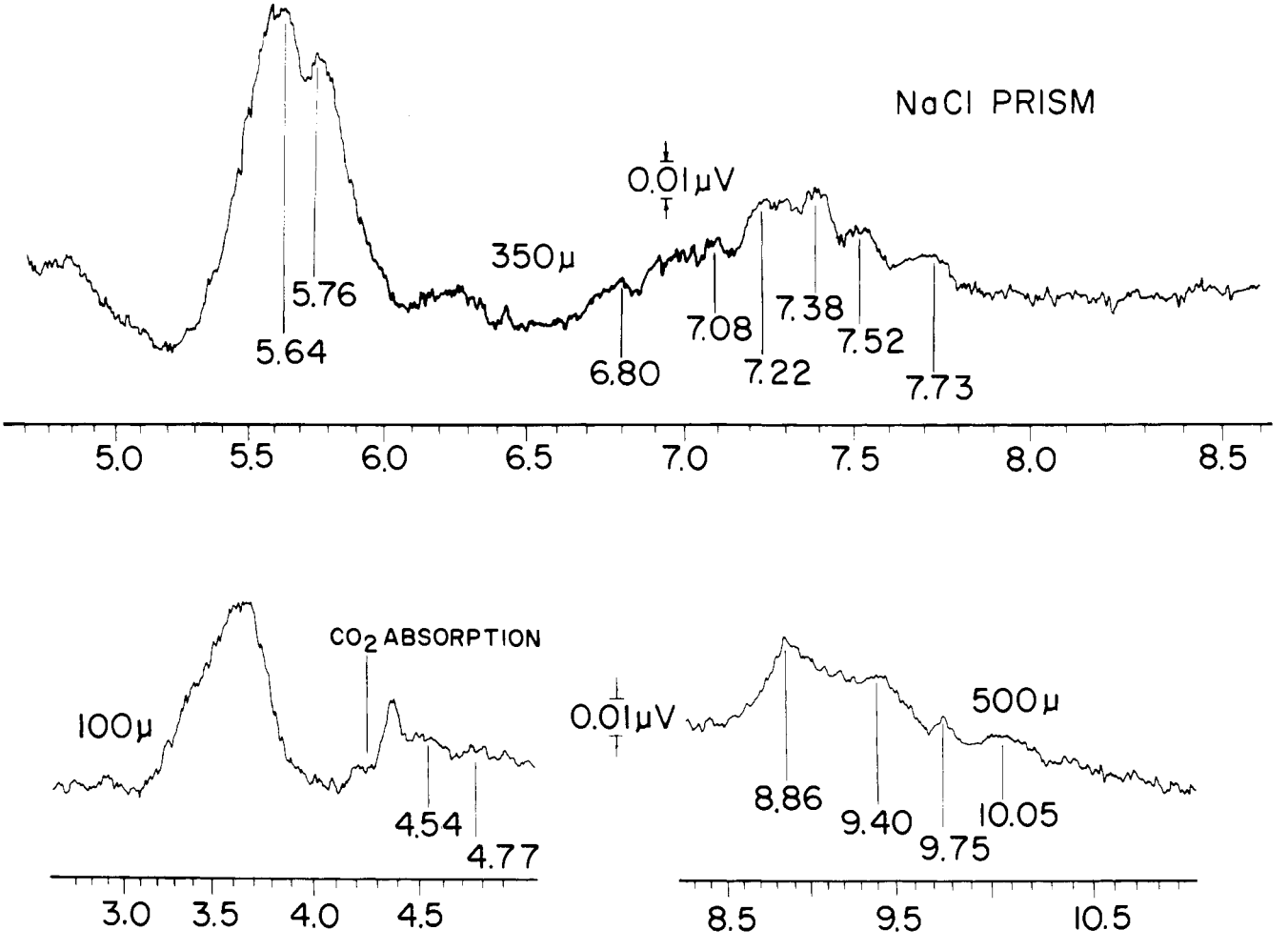

Figure 8. Emission spectrum of acetaldehyde-air first-stage cool flame from 2.7 to 10.9 microns

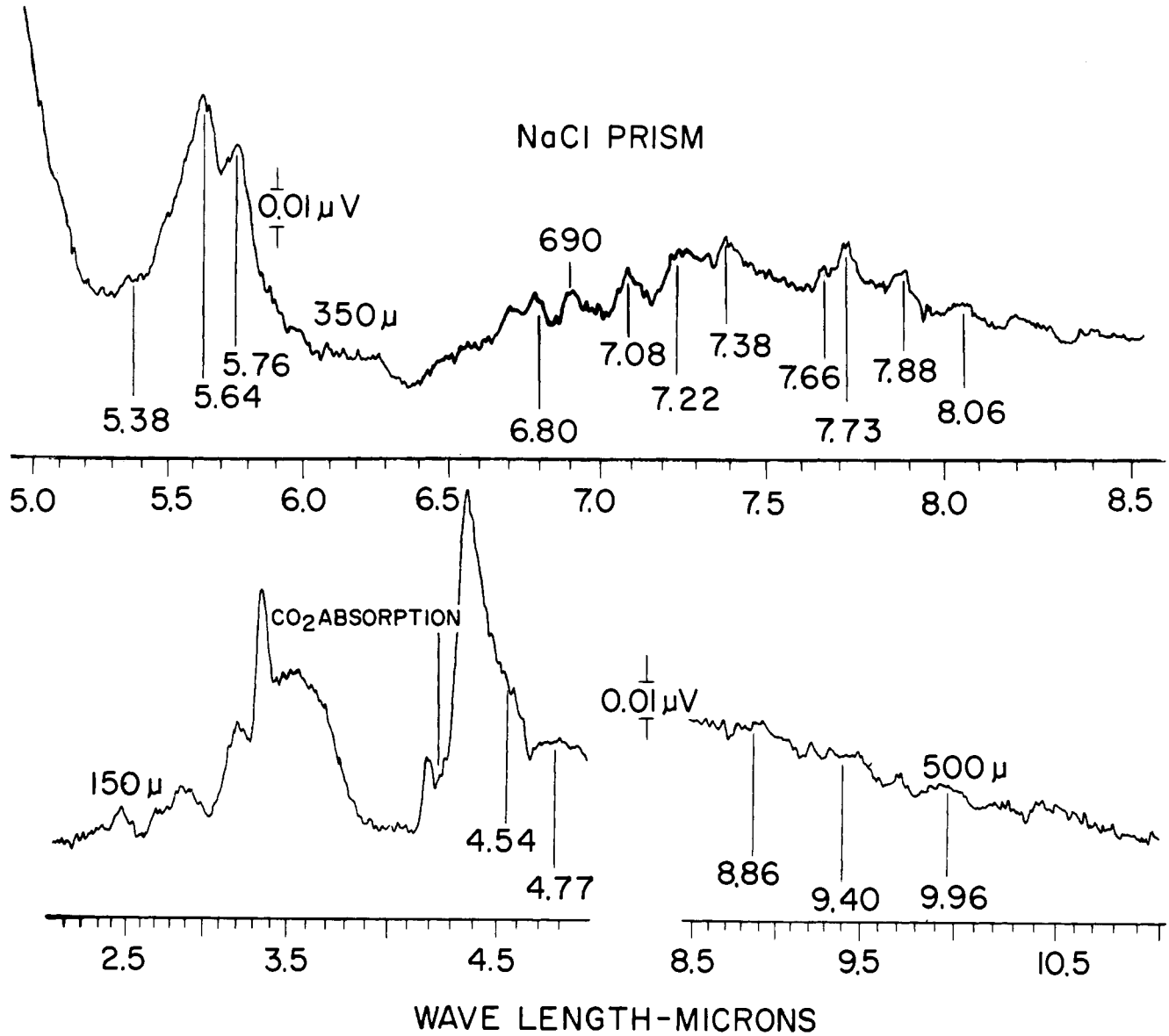

Figure 9. Emission spectrum of acetaldehyde-air second-stage flame from 2.1 to 11.0 microns

that the decrease in the intensity of the 3.6 micron radiation shown in Figure 5 indicates consumption of the aldehydes higher than formaldehyde.

Spectral Range 4.0 to 5.4 Microns. In this spectral range radiation from carbon dioxide and carbon monoxide was observed, in addition to a band near 4.85 microns with diethyl ether as the fuel. The 4.85-micron band was strongest in the second-stage of the diethyl ether flames (Figure 4). This radiation may result from dimethyl ether, which is known to have a strong band in absorption at 4.8 to 5.0 microns. There is also evidence for this species in the first-stage cool flame of diethyl ether (Figure 3). This band was not observed with either acetaldehyde or *n*-heptane fuel, which supports its identification as dimethyl ether.

Emission from carbon dioxide is attenuated by atmospheric absorption at 4.25 microns; this results in two peaks from carbon dioxide at approximately 4.2 and 4.4 microns. In the first-stage cool flame spectra considerable carbon dioxide emission was observed with diethyl ether and acetaldehyde (Figures 3 and 8), but it was almost unobservable with *n*-heptane (Figure 12). In the second-stage spectra, the carbon dioxide radiation was quite strong with diethyl ether and acetaldehyde but very weak with *n*-heptane (Figures 4, 9, and 13, respectively). Radiation from carbon monoxide is characterized by the peaks near 4.54 and 4.77 microns. While carbon monoxide radiation was relatively weak in the case of *n*-heptane, it was stronger than the carbon dioxide radiation; for the other two fuels the carbon dioxide radiation was much stronger than the carbon monoxide radiation.

Spectral Range 5.4 to 6.0 Microns. This range includes the strong emission from the carbonyl linkage, and in respect to the difficulty of identification of transient intermediates, it is similar to the 3.5-micron C — H stretching range.

In general, aldehydes, ketones, acids, esters, lactones, peroxides, and anhydrides are the most likely emitters in this region, and the information on absorption spectra given by Bellamy (*3*) indicates three rough groupings. Anhydrides and acyl peroxides might be expected between 5.4 and 5.7 microns; saturated aldehydes and esters might appear at 5.75 to 5.8 microns; and ketones, acids, lactones, and unsaturated aldehydes might emit between 5.8 and 6.0 microns. Evidence for each of these groups appears in the spectra.

Spectra in the various flame stages for diethyl ether, acetaldehyde, and *n*-heptane are shown in Figures 6, 11, and 15, respectively.

The diethyl ether flame in Figure 6 shows a band peak at 5.85 microns which does not appear with the other fuels. Diethyl ether itself has no band here, so the radiation must result from a product molecule. The strong peak at 5.74

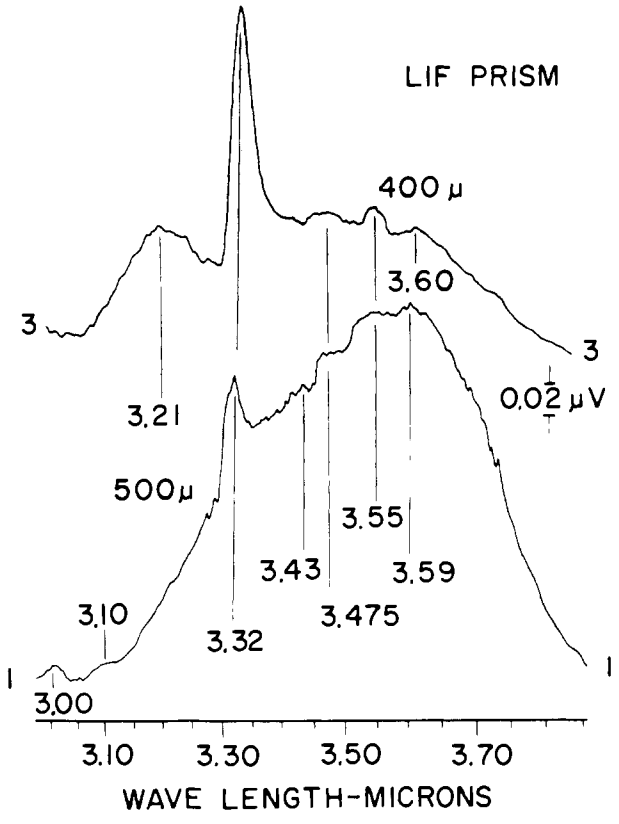

Figure 10. Emission spectra of acetaldehyde-air two-stage flame from 3.0 to 3.8 microns

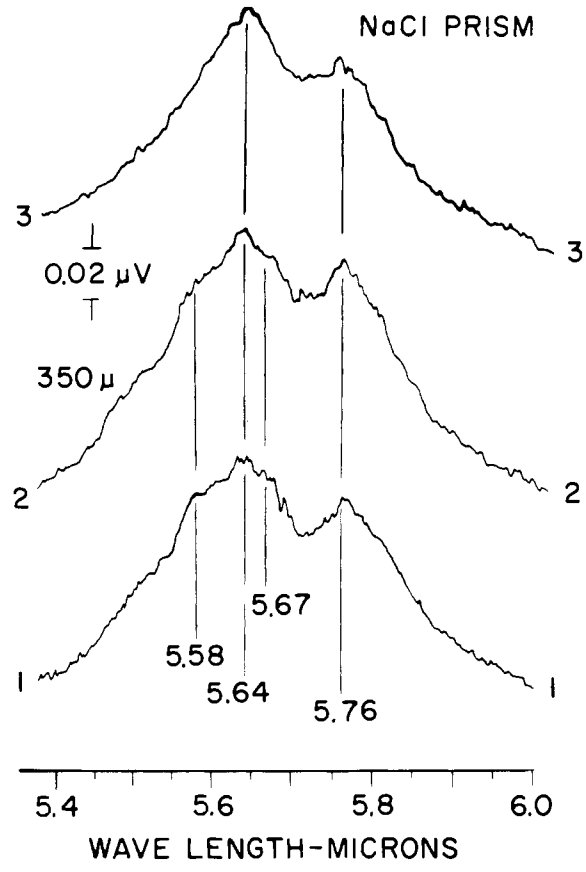

Figure 11. Emission spectra of acetaldehyde-air two-stage flame from 5.4 to 6.0 microns

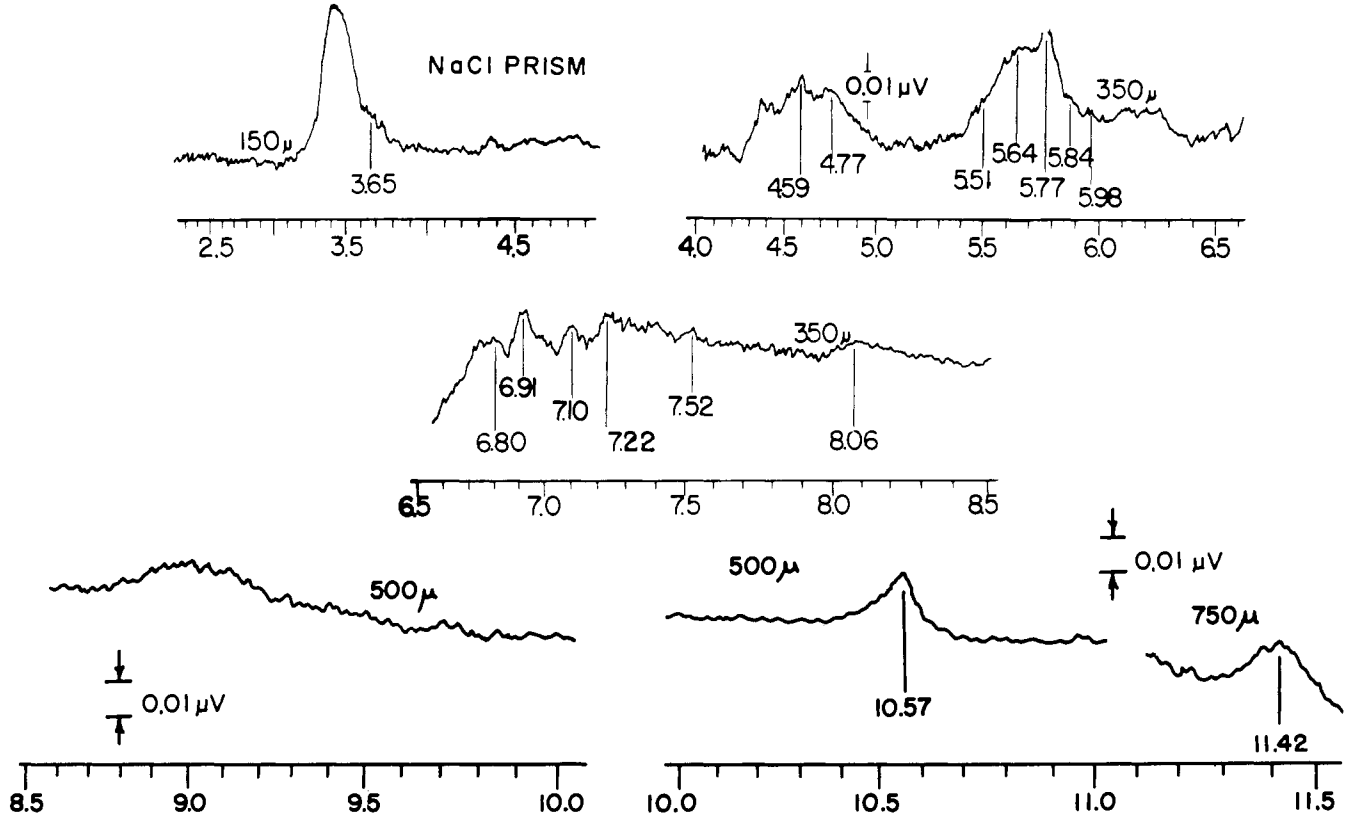

Figure 12. Emission spectrum of *n*-heptane-air first-stage cool flame from 2.3 to 11.5 microns

microns is probably from aldehydes which are apparently in highest concentration in zone 2 (between the first and second-stage flame fronts). On the other hand, the 5.5- to 5.7-micron region (anhydrides and peroxides, perhaps) grows relatively stronger in progressing from zone 1 to zone 4.

With acetaldehyde (Figures 8, 9, and 11) the 5.76-micron band, which is probably due at least partly to the original fuel, decreased somewhat in intensity in the second-stage flame. The 5.64-micron band intensity followed that of the 5.76-micron peak closely, but the secondary maxima at 5.58 and 5.67 microns disappeared in the second-stage flame.

The dominant feature in this portion of the heptane flame (as with ether) was the 5.77-micron region. The *n*-heptane flame spectrum also resembled that of ether in that the intensity in the range 5.5 to 5.6 microns tended to increase relative to that at 5.75 microns in progressing from the first-stage cool flame to the second-stage flame.

Spectral Range 6.0 to 8.5 Microns. In this spectral range, atmospheric water vapor absorption complicates the interpretation, but the interference is only serious at wave lengths shorter than 7.4 microns.

A number of emission peaks were observed in this spectral range. In the ether spectra (Figures 3 and 4) the strongest bands at 7.30 and 7.32 microns are very probably due to the symmetrical C—CH_3 deformation frequency in the fuel molecule. Similarly, the asymmetrical C—CH_3 fuel molecule deformation frequency may be responsible for the bands marked 6.96 and 6.89 microns, the discrepancy in wave lengths between the first and second-stage flames probably being due to inaccuracies caused by atmospheric water vapor absorption. The strong band at 7.81 microns in Figure 4 is believed to be emission from formaldehyde. The increase in intensity of this band as a function of flame position in the ether flame can be seen more clearly in Figure 7. The 7.95-micron band in Figures 4 and 7 is also probably a part of the formaldehyde system.

In the acetaldehyde spectra (Figures 8 and 9) bands appeared at 7.52 and 7.73 microns in the first-stage cool flame. The 7.73-micron band persisted in the second-stage flame whereas the 7.52-micron band did not. Also, in the second-stage flame new peaks appeared at 7.66, 7.88, and and 8.06 microns.

With *n*-heptane as fuel (Figures 12 and 13) the situation with respect to the acetaldehyde bands was different. The 8.06-micron band appeared in the first-stage cool flame. This band did not appear in the second-stage spectrum, but the 7.73- and 7.88-micron bands did appear. There is a slight indication for the presence of the 7.52-micron band in both spectra for *n*-heptane.

The 7.81-micron band, which was so prominent in the ether spectra (Figures 4 and 7), is not present in any of the spectra for the other two fuels (Figures 8, 9, 12, and 13), a fact which is rather surprising in the case of acetaldehyde.

Finally, minor peaks, such as those at 7.02, 7.08, 7.11, and 7.22 microns in Figures 4, 8, 9, and 13, are believed to be real, but assignment is difficult because of interference from atmospheric water vapor absorption.

Spectral Range 8.5 to 11.5 Microns. The strong band at 8.96 microns (Figures 3, 4, and 7) is undoubtedly due to emission from hot diethyl ether. The decrease in intensity in the successive spectra shown in Figure 7 would correspond to increased fuel consumption. Similarly the rather

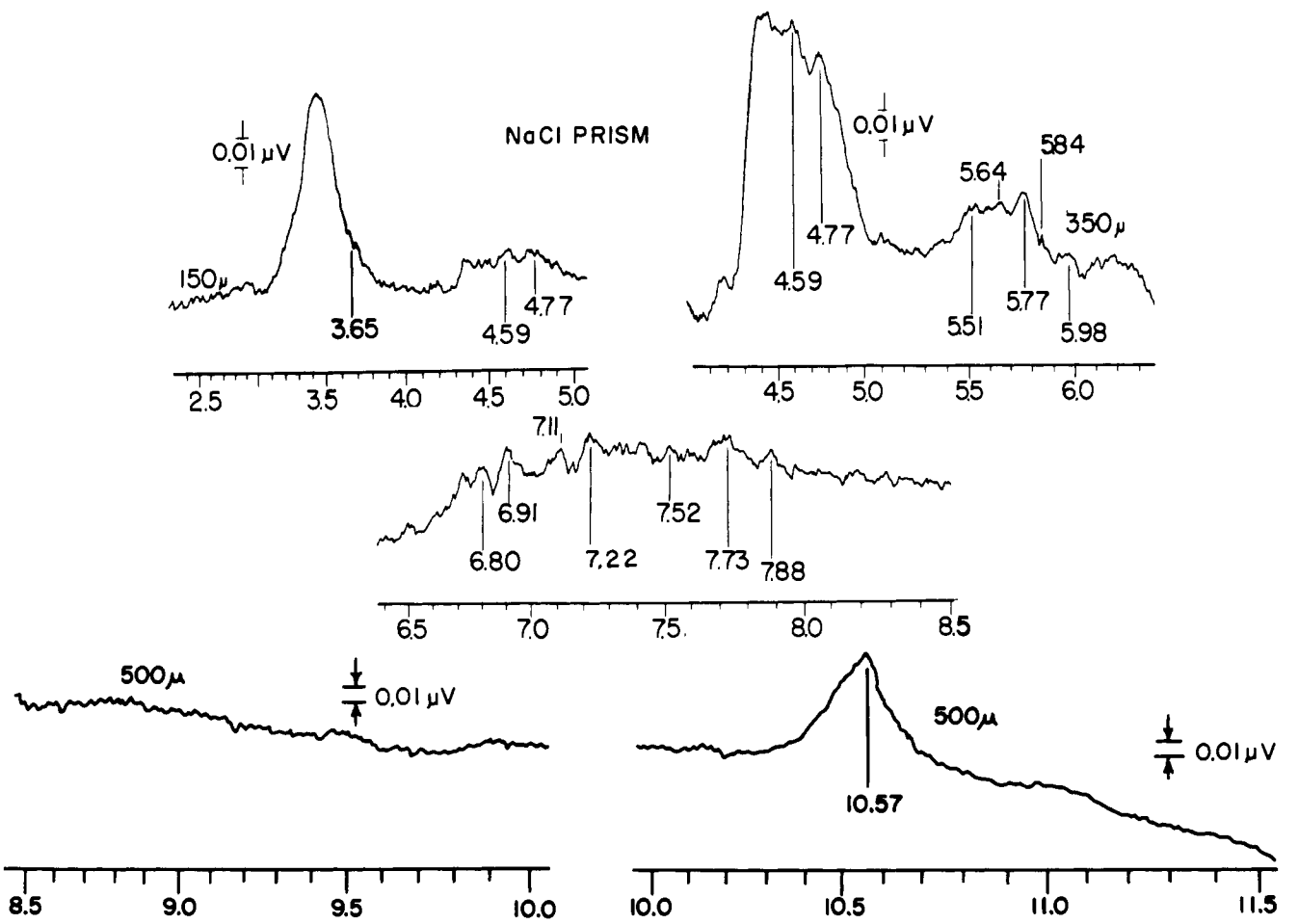

Figure 13. Emission spectrum of *n*-heptane-air second-stage flame from 2.4 to 11.5 microns

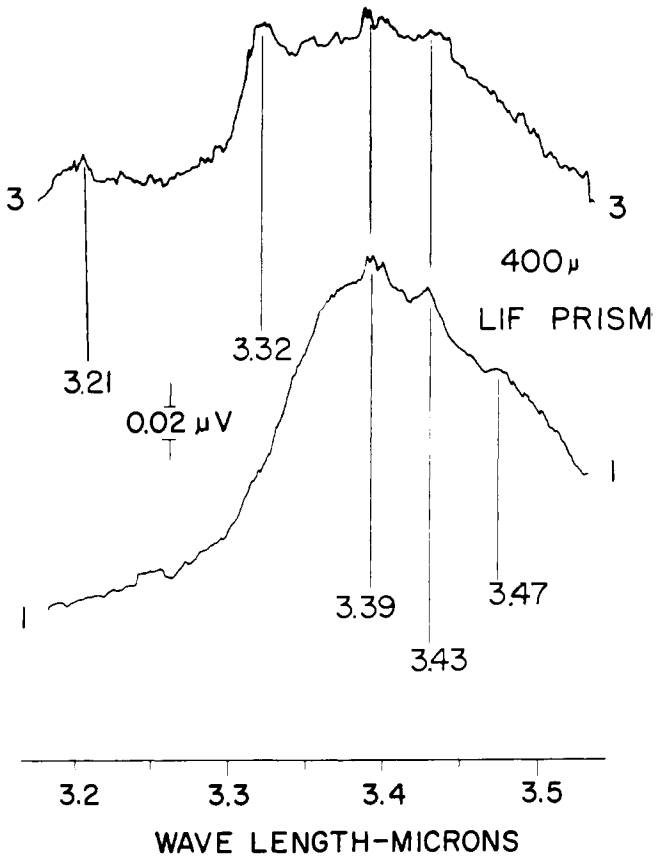

Figure 14. Emission spectra of *n*-heptane-air two-stage flame from 3.2 to 3.5 microns

strong band at 8.86 microns in Figure 8 is believed to be due to heated acetaldehyde; it is much weaker in the second-stage flame (Figure 9).

The bands at 9.4 and 9.5 microns in Figures 3, 4, 7, 8, and 9, may be due to emission from primary alcohols; both methyl and ethyl alcohol have strong absorption bands near 9.5 microns. Weak emission was observed in the vicinity of 10 microns in both stages of the acetaldehyde flame and in the second-stage flame of diethyl ether (Figures 4, 8, and 9). No assignment has been made for the 9.75-micron band in Figure 8, a remnant of which can be seen in Figure 9.

A band was observed at 10.57 microns with ether as the fuel (Figures 3, 4, and 7); and with *n*-heptane as the fuel (Figures 12 and 13). This band is very probably due to emission from ethylene.

In Figure 7, the ethylene concentration, as indicated by the intensity of the 10.57-micron band, increases in progressing from flame zone 1-1 to flame zone 3-3, reaches a maximum in zone 3-3 (the second-stage flame) and then decreases.

With *n*-heptane as the fuel (Figures 12 and 13) the ethylene radiation again was stronger in the second-stage flame than in the first-stage cool flame. Also a band at 11.42 microns appeared in the *n*-heptane first-stage cool flame but was not present in the second-stage flame. Of the three fuels tested, only acetaldehyde showed no evidence for the presence of ethylene radiation at 10.57 microns.

Spectral Range 11.5 to 14.0 Microns. Only diethyl ether gave detectable emission bands in this spectral range (Figures 3 and 4). Weak emission bands were observed at 11.03, 11.79, 12.11, 12.30, 12.43, 13.07, 13.32, 13.48, 13.74, and 13.96 microns in the second-stage flame and at 13.75 microns in the first-stage cool flame. No specific emitters have as yet been assigned to any of these bands except the band at 13.74 microns which may be due to acetylene. Some of these bands may be due to organic peroxides which are known to have absorption bands between 11.2 and 12.2 microns.

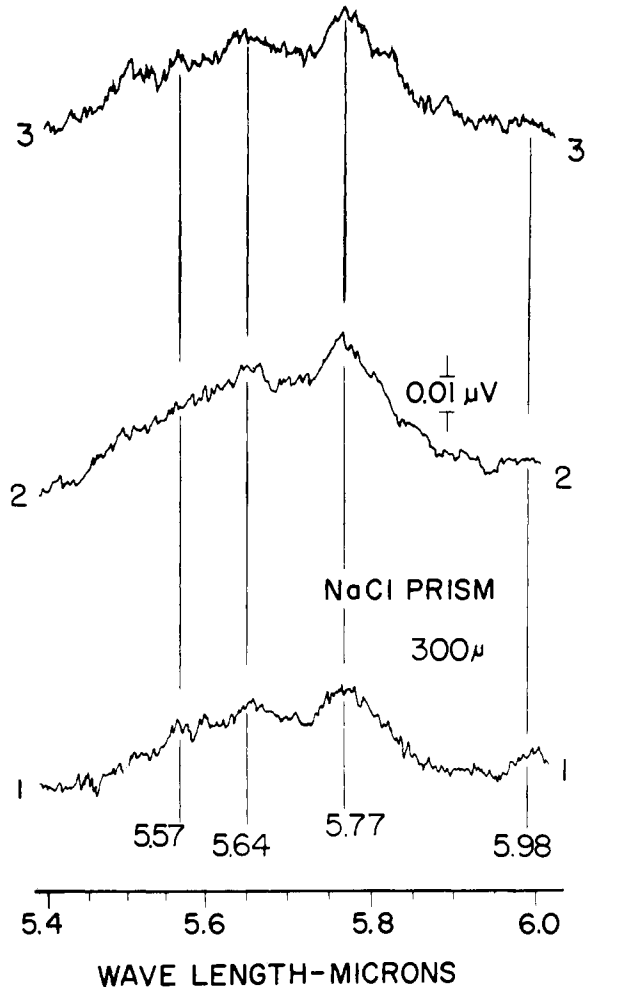

Figure 15. Emission spectra of *n*-heptane-air two-stage flame from 5.4 to 6.0 microns

For purposes of comparison, the wave lengths at which maxima were observed in the emission spectra of the three fuels tested are listed in Table I.

CONCLUSIONS

Although the over-all aim of this work is to understand the reaction kinetics of low temperature oxidation, the data presented permit little speculation as to the actual sequence of the reactions. However, a number of intermediate products of the reactions have been identified from the infrared spectra. Formaldehyde, ethylene, carbon dioxide, carbon monoxide, and water vapor were identified with reasonable certainty; other possible emitters were dimethyl ether, ketones, acids, esters, lactones, anhydrides, aldehydes, peroxides, primary alcohols, and acetylene. Several specific observations were made.

The ratio of carbon monoxide concentration to carbon dioxide was higher in the case of *n*-heptane than with either of the other two fuels in all stages of the low temperature reactions.

Formaldehyde was present in increasing amounts as the diethyl ether reaction was traversed from the first-stage cool flame through the second-stage. No unambiguous evidence for formaldehyde was present in the case of *n*-heptane and acetaldehyde.

With diethyl ether as the fuel, ethylene was formed readily and reached a maximum emission in the second-stage flame. Ethylene was also detected with *n*-heptane as the fuel, and again the emission was greater in the second-stage flame than in the first-stage cool flame. No ethylene was detected with acetaldehyde as the fuel.

Table I. Maxima Observed in Infrared Emission Spectra of Two-Stage Flames of Diethyl Ether, Acetaldehyde, and *n*-Heptane in Air

Wave Length, Microns					
Diethyl Ether		Acetaldehyde		*n*-Heptane	
First-stage cool flame	Second-stage flame	First-stage cool flame	Second-stage flame	First-stage cool flame	Second-stage flame
	3.20		3.21		3.21
3.35	3.32	3.32	3.32		3.32
3.38	3.38			3.39	3.39
3.43	3.46	3.43		3.43	3.43
		3.475	3.475	3.47	
3.52		3.55	3.55		
3.60		3.59	3.60	3.65	3.65
		4.54	4.54	4.59	4.59
4.85	4.85	4.77	4.77	4.77	4.77
				5.51	5.51
5.59	5.59	5.58		5.57	5.57
		5.64	5.64	5.64	5.64
5.67	5.67				
5.74	5.74	5.76	5.76	5.77	5.77
5.85	5.85				
				5.98	5.98
		6.80	6.80	6.80	6.80
	6.89		6.90	6.91	6.91
6.96	7.02	7.08	7.08		
		7.22	7.22	7.22	7.22
7.30	7.32	7.38	7.38		
	7.47	7.52		7.52	7.52
			7.66		
		7.73	7.73		7.73
7.81	7.81				
			7.88		7.88
	7.95				
			8.06	8.06	
		8.86	8.86		
8.96	8.96				
		9.40	9.40		
9.50	9.50				
		9.75			
	9.99	10.05	9.96		
10.57	10.57			10.57	10.57
	11.03				
				11.42	
	11.79				
	12.11				
	12.30				
	12.43				
	13.07				
	13.32				
	13.48				
13.75	13.74				
	13.96				

There was evidence for the formation of dimethyl ether with diethyl ether as the fuel.

Some of the variation in intensity of the various bands is undoubtedly due to temperature variation in the various flame zones. The temperature in the second-stage ether flame is known to be approximately 1000° K. as compared to about 750° K. in the first-stage cool flame (*4*).

Eventual identification of other emission bands, such as those at 7.52, 7.73, 7.88, 8.06, and 11.4 microns, will further define intermediate species which should contribute to the understanding of the reaction mechanism. More work must be done toward identification of these unknown bands. Such identification will be facilitated by improvements on the burner geometry and optical system which will increase the intensity of the emission spectra. Also, both emission and absorption data will be taken in future studies. Identification of emitters will be implemented by studying emission and absorption spectra of pure known compounds alone and in the presence of varying amounts of oxygen.

The effect of additives on flame structure and emission and absorption spectra should be studied. Such research should provide useful information concerning the reaction mechanism for the oxidation of hydrocarbons and have practical application in affording a better understanding of the relationship between the occurrence of low temperature reactions (cool and second-stage flames) and knock in the internal combustion engine.

LITERATURE CITED

(1) Agnew, W. G., Agnew, J. T., *Ind. Eng. Chem.* **48**, 2224 (1956).
(2) Agnew, W. G., Agnew, J. T., Wark, K., "Fifth Symposium on Combustion," p. 766, Reinhold, New York, 1955.
(3) Bellamy, L. J., "Infrared Spectra of Complex Molecules," Wiley, New York, 1954.
(4) Donovan, R. E., Agnew, W. G., *J. Chem. Phys.* **23**, 1592 (1955).
(5) Egerton, A. C. G., Thabet, S. K., *Proc. Roy. Soc.* **A211**, 445 (1952).
(6) Fox, J. J., Martin, A. E., *Ibid.*, **A175**, 208 (1940).
(7) Powling, J., *Fuel* **28** (1940).

Received for review March 22, 1957. Accepted August 1, 1957.